

UC Davis

UC Davis Previously Published Works

Title

Synbiotics Bifidobacterium infantis and milk oligosaccharides are effective in reversing cancer-prone nonalcoholic steatohepatitis using western diet-fed FXR knockout mouse models

Permalink

<https://escholarship.org/uc/item/16r9k3pd>

Authors

Jena, Prasant Kumar
Sheng, Lili
Nagar, Nidhi
et al.

Publication Date

2018-07-01

DOI

10.1016/j.jnutbio.2018.04.007

Peer reviewed



Published in final edited form as:

J Nutr Biochem. 2018 July ; 57: 246–254. doi:10.1016/j.jnutbio.2018.04.007.

Synbiotics *Bifidobacterium infantis* and milk oligosaccharides are effective in reversing cancer-prone non-alcoholic steatohepatitis using Western diet-fed FXR knockout mouse models

Prasant Kumar Jena^{1,¥}, Lili Sheng^{1,¥}, Nidhi Nagar¹, Chao Wu³, Daniela Barile⁴, David A. Mills^{4,5}, and Yui-Jui Yvonne Wan^{1,*}

¹Department of Pathology and Laboratory Medicine, University of California, Davis, Sacramento, CA, USA

³Research and Development, Hilmar Ingredients, Hilmar, CA, USA

⁴Department of Food Science and Technology, University of California, Davis, CA, USA

⁵Department of Viticulture and Enology, University of California, Davis, CA, USA

Abstract

Prebiotic milk oligosaccharides (MO) are complex sugars that selectively enhance the growth of *Bifidobacterium infantis* (*B. infantis*). The current study examines the effects of bovine MO and *B. infantis* in preventing non-alcoholic steatohepatitis (NASH) in Western diet (WD)-fed bile acid (BA) receptor FXR (farnesoid × receptor) knockout (KO) mice. WD-fed FXR KO mice, which have cancer-prone NASH and reduced *B. infantis*, were supplemented with *B. infantis*, MO, and combination of both. Two months intervention by *B. infantis* and/or MO improved insulin sensitivity. In addition, all 3 treatments reduced expression of pro-inflammatory genes in the liver and ileum. Consistently, 7 months treatment reduced hepatic lymphocyte infiltration in WD-fed FXR KO mice. In addition, *B. infantis*, but not MO, decreased hepatic triglyceride and cholesterol. A combination of both further reduced hepatic cholesterol, the precursor of BAs, but not hepatic triglyceride. All three treatments modulated hepatic and serum BA profile by reducing deoxycholic acid, hyodeoxycholic acid and increasing chenodeoxycholic acid as well as ursodeoxycholic acid level. In addition, *B. infantis* and MO decreased hepatic CYP7A1 and increased the expression of *Sult2a1*, *Sult2a2*, and *Sult2a3* suggesting decreased BA synthesis and

Corresponding Author: Yu-Jui Yvonne Wan, Ph.D., Room 3400B, Research Building III, 4645 2nd Ave, Sacramento, CA 95817, USA, Department of Pathology and Laboratory Medicine, University of California, Davis Health Systems, Tel: 916-734-4293, Fax: 916-734-3787, yjywan@ucdavis.edu.

[¥]These authors contributed equally to this work

Contributors: YJW designed the study; PKJ, LS, and NN performed experiments, PKJ, LS, NN, CY, DB, DAM, and YJW analyzed and interpreted the data; PKJ, LS, and YJW wrote the manuscript; all authors commented and approved the final manuscript.

Provenance and peer review: Not commissioned; externally peer reviewed.

Competing interests: The authors of this paper declare that they do not have any disclosures regarding funding or conflict of interest.

Publisher's Disclaimer: This is a PDF file of an unedited manuscript that has been accepted for publication. As a service to our customers we are providing this early version of the manuscript. The manuscript will undergo copyediting, typesetting, and review of the resulting proof before it is published in its final citable form. Please note that during the production process errors may be discovered which could affect the content, and all legal disclaimers that apply to the journal pertain.

increased detoxification. Furthermore, *B. infantis* and MO increased ileal BA membrane receptor TGR5 as well as *Glp1r*, *PC1/3*, and *Nos3* suggesting increased TGR5-regulated signaling. Moreover, MO alone, but not *B. infantis*, could increase the abundance of butyrate-generating bacterium that has beneficial effect in NASH treatment. Together, *B. infantis* and MO have their unique and combined effects in reversing NASH in WD-fed FXR KO mice.

Keywords

Probiotics; prebiotics; microbiota; liver cancer; bile acid; dysbiosis; TGR5

1. Introduction

Bifidobacteria have co-evolved with humans, and it appears to be beneficial to the well-being of infants [1]. Specifically, *Bifidobacterium longum* subsp. *infantis* (*B. infantis*) has intestinal and extra-intestinal health benefits [2]. *B. infantis* modulates gut barrier functions and protects epithelial cells against cytokine or chemical-induced inflammation [3, 4]. In addition, *B. longum* is effective in preventing allergic pathologies, psoriasis, and chronic fatigue syndrome [2, 5]. Moreover, other *Bifidobacterium* spp. has anti-obesity effect and can improve alcohol-induced liver injury [6]. During evolution, *B. infantis* acquired an ability to metabolize human milk oligosaccharides (MO) that are complex sugar and nutrient for newborns [7, 8]. Additionally, MO enhance the growth of *Bifidobacteria* and *Lactobacilli* at the expense of potentially harmful bacteria such as *Clostridia*, *Enterococci*, *Eubacteria*, and *Enterobacteria* creating an acidic environment that is less favorable to pathogens [9–11]. Thus, the synbiotics containing probiotics *B. infantis* and prebiotics MO have added health benefits. For example, *B. infantis* plus MO are effective in inducing the expression of genes involved in integrity of barrier function [14]. They also have anti-inflammatory effect in the intestinal epithelial cells [12]. Moreover, growing evidence indicate that breast milk in neonates as well as MO are beneficial to intestinal health [13]. Therefore, breast-fed infants have reduced intestinal permeability compared to formula-fed infants [14]. Because gut dysbiosis contribute to hepatic inflammation [15–18], we hypothesize that synbiotics *B. infantis* plus MO may have beneficial effects in protecting against the development of non-alcoholic steatohepatitis (NASH) caused by dysregulated bile acid (BA) synthesis and dysbiosis.

BAs are essential for lipid and carbohydrate metabolism and play a significant role in regulating host immunity and inflammation [18, 19]. Activation of farnesoid × receptor (FXR) by BAs, protects the distal small intestine from bacterial invasion and overgrowth in bile duct ligation in mouse models [20]. Activation of FXR also has beneficial effects against metabolic disorders [21, 22]. In addition, FXR agonists have promising effect in NASH treatment as revealed in clinical trials [23]. In metabolic disease mouse models, feeding wild type mice with a Western diet (WD) will not produce liver cancer in their lifetime. In contrast, mice lacking FXR develop steatosis, NASH, and liver cancer spontaneously, and WD-feeding facilitates the liver carcinogenesis process [24–26]. Consistently, patients with severe cirrhosis and liver cancer have reduced hepatic FXR [26, 27]. Moreover, dysregulated bile acid synthesis is frequently found in patients who have

metabolic diseases including liver cancer. Together, FXR knockout (KO) mice are human relevant models that are useful to study the prevention and treatment of liver carcinogenesis.

It is known that dysregulated BA synthesis is always accompanied by dysbiosis because BAs are generated by host and bacterial enzymes [18, 28, 29]. Our published data have already uncovered specific BAs and gut microbiota that contribute to the development of NASH leading to cancer formation in FXR KO mouse models [15–17]. In the current study, we investigated a hypothesis that through modulating BA synthesis, synbiotics *B. infantis* plus bovine MO are effective in preventing the development of NASH. Our novel data revealed the beneficial effects of *B. infantis* and MO in reversing cancer-prone NASH in WD-fed FXR KO mice.

2. Materials and Methods

2.1. Bacterial culture condition

B. infantis (ATCC 15697, Manassas, VA, USA) were grown in a food grade facility and stored at -80°C [30]. The purity and viability of the bacteria were confirmed every 6 months; they were grown anaerobically at 37°C in a semisynthetic de Man, Rogosa, Sharpe broth (Becton Dickinson, Franklin Lakes, NJ, USA) supplemented with 1% (wt/vol) L-cysteine hydrochloride. After centrifugation, bacteria were suspended in saline before oral administration via gavage.

2.2 Bovine MO production and characterization

A product enriched in MO was supplied by Hilmar Ingredients (Hilmar, CA, USA). Bovine MO were concentrated and purified from commercially available whey permeate using a series of ultrafiltration and chromatographic steps. Lactose was partially removed by concentration, crystallization, and precipitation. The lactose and mineral reduced permeate was treated by an adsorption column containing 100 liters of functionalized copolymer of styrene and divinyl benzene to remove color in the stream. MO in the decolorized stream was further concentrated using a single stage ultrafiltration membranes (Molecular weight cut off of 1000 Dalton) to remove minerals and lactose in the solution. The final concentrate was freeze-dried and stored in a vacuum desiccator at room temperature. The total carbohydrate composition of MO was determined using an Agilent 6520 accurate-mass Q-TOF LC/MS with a microfluidic nano-electrospray chip according to previously published methods [31]. The MO profile of this product was consistent with a previously formulated supplement that has been used in a human clinical study [32]. The concentration of lactose and select MO was measured using a high-performance anion-exchange chromatography with pulsed amperometric detection (Thermo Scientific HPAEC-PAD ICS-5000, Sunnyvale, CA, USA). See supplemental information (Supplementary Table S1).

2.3. Mice

Specific pathogen-free C57BL/6 wild type (WT) mice (Jackson Laboratory, Sacramento, CA, USA) as well as age- and sex-matched FXR KO mice [33] were housed in steel microisolator cages at 22°C with a 12-hour light/dark cycle. They were given a WD containing 21.2% fat, 34% sucrose, and 0.2% cholesterol (Envigo, Indianapolis, IN, USA)

right after weaning (3 weeks, 6–10 mice per group). For interventions, mice were given *B. infantis* (10^9 cfu per mouse, orally, once a week) in saline, bovine MO (7% in a diet that lacks 7% cellulose), or a combination of *B. infantis* plus MO while mice continued a WD. For short-term study, 3-month old mice were treated for 2 months and euthanized when they were 5-month old. For long-term study, 3-month old male mice were treated for 7 months and euthanized when they were 10-month old. Experiments were conducted in accordance with the National Institutes of Health Guidelines for the Care and Use of Laboratory Animals under protocols approved by the Institutional Animal Care and Use Committee of the University of California, Davis.

2.4. Biochemical assays and histology

Serum alanine aminotransferase (ALT; Pointe Scientific, Canton, MI, USA), serum alkaline phosphatase (ALP; Pointe Scientific), hepatic triglyceride, and hepatic cholesterol (BioAssay Systems, Hayward, CA, USA) levels were quantified according to the manufacturer's instructions. Hematoxylin and eosin stained liver tissues were subjected to histology analysis. Steatosis score was graded on a scale of 0 (<5%), 1 (5%–33%), 2 (34%–66%), and 3 (>66%), and hepatic lymphocyte infiltration score was graded on a scale of 0 (absent), 1 (rare), 2 (mild), 3 (moderate), and 4 (severe).

2.5 Bile acid quantification

Frozen liver tissues (50 mg) were homogenized in cold methanol/internal standard solution (100 μ l internal standard solution and 500 μ l methanol). Serum samples (50 μ l) were added to 500 μ l of cold methanol and 100 μ l of internal standard based on published methods [15–17, 34–36]. After centrifuge, the supernatant was dried in a Savant speedvac concentrator (Thermo Scientific, Rockford, IL, USA). The residue was then reconstituted by adding 50 μ l of methanol: water (50:50, v/v) followed by centrifugation at 10,000 g for 1 min at 4°C. The supernatants were used for BA quantification. The detection of BAs was carried out on a Prominence™ UFLC system (Shimadzu, Kyoto, Japan) coupled to an API 4000 QTRAP™ mass spectrometer (ABSciex, Redwood City, CA, USA) operated in the negative ionization mode. Chromatography was performed on a Kinetex C₁₈ column (50 mm \times 2.1 mm, 2.6 μ m) maintained at 40°C preceded by a high-pressure column prefilter. The mobile phase consisted of a gradient of methanol delivered at a flow rate of 0.4 ml/min. Mass Spectrometer parameters were described in our publications [35].

2.6. Mouse gene expression and quantification of bacterial genes

RNA was isolated using TRIzol (Invitrogen, Carlsbad, CA, USA) and reverse transcribed into cDNA. qRT-PCR was performed on an ABI 7900HT Fast real-time PCR system using Power SYBR Green PCR Master Mix (Applied Biosystems, Foster City, CA, USA). Primers sequences are available in supplementary table S2. The mRNA levels were normalized to the level of *Gapdh* mRNA.

For bacterial gene quantification, DNA was extracted from cecal content (0.05 gram) using ZR Fecal DNA MiniPrep Kit (Zymo Research, Irvine, CA, USA), quantified by NanoDrop (Thermo Scientific, Wilmington, DE, USA), and amplified using primers (Supplementary table S2) based on the published sequences [15, 37–41]. A dissociation step was included to

analyze the melting profile of amplified products. In parallel, qPCR was done using ten-fold serial diluted synthetic DNA fragments (Integrative DNA technologies, Redwood city, CA, USA) of a bacterial gene with known concentrations. Bacterial DNA concentration was calculated using standard curves of diluted synthetic DNA fragment based on published methods [42].

2.7. Protein extraction and quantification

Proteins were extracted (30 mg) by T-PER protein extraction reagent (Thermo Scientific, Rockford, IL, USA) with protease and phosphatase inhibitor cocktail (Thermo Scientific, Rockford, IL, USA) followed by protein quantification using protein bicinchoninic acid assay reagent (Thermo Scientific, Rockford, IL, USA). Hepatic protein (40 µg) was subjected to polyacrylamide gel electrophoresis under reducing conditions followed by transfer to polyvinylidene difluoride membranes. The membranes were incubated with 4% non-fat milk followed by an antibody. The following primary antibodies (catalogue number and dilutions) were used: CYP7A1 (MABD42, 1:1000, Merck, Temecula, CA, USA), CYP8B1 (TA313734, 1:1000, Origene Technologies, Rockville, MD, USA), SULT2A1 (OABF01591, 1:1000, Aviva systems, San Diego, CA, USA), and β-ACTIN (A1978, 1:10000; Sigma Chemical Co, St Louis, MO, USA).

Membranes were then incubated with horseradish peroxidase-conjugated secondary antibodies. The signals were detected using an ECL enhanced chemiluminescence system with Pierce SuperSignal West Pico chemiluminescent substrates (Thermo Fisher Scientific, Rockford, IL, USA).

2.8. Statistical analysis

Unpaired Student's *t*-test and one-way analysis of variance were performed using Prism 6.0 (GraphPad, La Jolla, CA, USA). Data are expressed as mean ± SD. *P*-values were adjusted for multiple comparisons using false discovery rate. *P* < 0.05 was considered statistically significant.

3. Results

3.1. *B. infantis* and MO improve insulin sensitivity and reduce hepatic inflammatory signaling in WD-fed FXR KO mice after 2-months treatment

Our published data revealed that feeding FXR KO mice with a WD facilitated the development of NASH that lead to liver carcinogenesis [16]. The current study reveals for the first time that FXR KO mice had reduced *B. infantis*. However, supplementation of either *B. infantis* or MO for two months increased the abundance of *B. infantis*. In addition, a combination of both further increased *B. infantis* compared with single supplementation (Figure 1A). Although FXR regulates carbohydrate homeostasis, FXR deficiency did not affect blood glucose level post insulin injection in 5-month old WD-fed mice. However, *B. infantis* and/or MO improved insulin sensitivity (Figure 1B, C). In addition, FXR deficiency elevated serum ALP and ALT levels, which were reduced by *B. infantis* and/or MO (Figure 1D–E).

By studying the expression of hepatic pro-inflammatory and pro-fibrotic genes, the data revealed that *Il1 β* , *Il6*, *Tnfa*, *Timp1*, *Mcp-1*, *Col1a1*, *Ccl17*, and *Ccl20*, which had increased expression level due to WD feeding and FXR inactivation, were reduced by 2 months of *B. infantis* and MO supplementation (Figure 2A).

Enterohepatic circulation of bile salts takes place in ileum, where expresses high level of FXR to regulate BA homeostasis. In addition, the liver receives 70% of its blood from the intestine and is constantly exposed to intestinal-derived metabolites. Moreover, our published data revealed that dysregulated BA homeostasis and gut dysbiosis contribute to the development of NASH [16,17]. Thus, gene expression was also studied in the ileum. Consistent with the data generated in the liver, the expression of ileal inflammatory genes, such as *Il1 β* , *Il6*, *Tnfa*, *Timp1*, *Mcp-1*, and *Inos*, were also reduced with *B. infantis* plus MO supplementation (Figure 2B). However, *B. infantis* or MO alone did not reduce the expression of several pro-inflammatory genes such as ileal *Il1 β* and *Inos*. Surprisingly, ileal *Il6* mRNA was induced by MO alone, but reduced by *B. infantis*. Further, ileal *Il10* and *Reg3 γ* , which were reduced with FXR deficiency, were increased by all three treatments.

3.2. *B. infantis* and MO prevent NASH in WD-FXR KO mice after a long-term 7 months treatment

Although 5-month old FXR KO mice had increased hepatic inflammatory signaling, liver histology did not reveal apparent inflammation [15]. Hepatic lymphocyte infiltration was only detected when WD-fed FXR KO male mice were 10 months old [16]. Thus, long-term 7 months intervention was performed to analyze whether *B. infantis* and MO could eliminate hepatic lymphocytes induced by dysregulated BA synthesis. Consistent with previous observation, 10-month old WD-fed FXR KO mice developed severe NASH with massive hepatic lymphocyte infiltration (Figure 3A, B). *B. infantis* and MO eliminated hepatic lymphocytes and reduced ALT level (Figure 3A–C). Moreover, *B. infantis* improved fat score, as well as hepatic triglyceride and cholesterol levels. In contrast, MO had no effect in reducing hepatic triglyceride or cholesterol (Figure 3D–F). Nevertheless, hepatic cholesterol was substantially reduced and became even lower than that of *B. infantis*-treated group when a combination of both was used (Fig. 3F).

Both short and long-term experiments revealed the impressive anti-inflammatory effect of *B. infantis* and MO in the liver. For examples, the expressions of hepatic and Ileal genes, such as *Il1 β* , *Il6*, *Ccl17*, *Ccl20*, *Cxcl10*, and *Ifn γ* , were induced in WD-fed FXR KO mice, but reduced by *B. infantis* and MO supplementation. In addition, WD intake and FXR KO-induced hepatic *Tnfa*, *Icam1*, *Il4*, *Timp1*, and *F4/80* mRNAs were reduced by *B. infantis* and MO intake. However, a combination of *B. infantis* plus MO had better effects in reducing the expression of hepatic *Foxp3* and inducing ileal *Reg3 γ* mRNA levels (Figure 4A–B).

3.3. *B. infantis* and MO modulate BA profile

Because elevated BA leads to liver carcinogenesis in FXR KO mice [25, 43–45], we studied the effect of *B. infantis* and MO on shifting BA profile. The data showed that *B. infantis* and MO normalized the concentration of certain BAs in 10-month old WD-fed FXR KO mice.

For example, FXR deficiency had opposite effects on changing hepatic and serum level of α -muricholic acid (α -MCA), β -muricholic acid (β -MCA) as well as taurodeoxycholic acid (TDCA), but *B. infantis* and/or MO treatments reversed those changes to a certain degree (Figure 5). In addition, increased hepatic and serum deoxycholic acid (DCA) and hyodeoxycholic acid (HDCA) found in WD-fed FXR KO mice were reduced by *B. infantis* and MO (Figure 5). However, *B. infantis* and MO increased hepatic chenodeoxycholic acid (CDCA) and tauroolithocholic acid (TLCA), which are the endogenous ligands of FXR and TGR5 (Takeda G protein coupled receptor 5) (Figure 5A). Another TGR5 ligand, hepatic lithocholic acid (LCA) was increased by *B. infantis* and a combination of *B. infantis* plus MO. Moreover, *B. infantis* plus MO were more effective in reducing hepatic DCA, HDCA, and CA (cholic acid), as well as inducing hepatic CDCA, LCA, and UDCA (ursodeoxycholic acid) than the single treatment. Furthermore, all three treatments reduced hepatic CA, but increased serum CA suggesting the effect of *B. infantis* and MO in redistribution of CA and increasing TCA (taurocholic acid) de-conjugation in the gut (Figure 5). It has been shown that FXR deficiency can increase TCA pool size [46]. Our data showed TCA was reduced in serum, but not changed in liver, in FXR KO mice, suggesting TCA might be spilled from the liver to other sites in WD-fed FXR KO mice. Moreover, *B. infantis* and/or MO reversed the changes of TCA and T- α , β -MCA (tauro- α , β -muricholic acid) in the serum caused by FXR deficiency.

3.4. *B. infantis* and MO affect BA synthesis

The expression of genes that regulate BA homeostasis was also shifted by *B. infantis* and MO treatment. For example, FXR deficiency-induced hepatic CYP7A1 was reduced by *B. infantis* and MO suggesting their effect in reducing hepatic CA synthesis (Fig. 6A, B). Only *B. infantis* reversed FXR deficiency-induced change of *Cyp8b1* at mRNA and protein level. In addition, FXR deficiency-reduced hepatic *Cyp7b1* and *Cyp39a1* were increased by *B. infantis* and MO supplementation (Figure 6A). Moreover, the level of hepatic SULT2A1, which was increased with FXR deficiency, was further increased by *B. infantis* plus MO treatment (Figure 6A, B). Consistently, the mRNA level of *Sult2a1*, *Sult2a2*, and *Sult2a3* was increased by FXR deficiency and further increased by a combination of *B. infantis* and MO treatment (Figure 6A). In contrast to all three isoforms of *Sult2a*, the hepatic mRNA level of *Sult2a8*, which was reduced with FXR deficiency, was further reduced by *B. infantis* alone (Figure 6A). Furthermore, the mRNA levels of *Sult2b1*, *Abcg5*, and *Abcg8* were reduced by FXR deficiency, and all three treatments reversed such reductions (Figure 6A). In the ileum, FXR deficiency reduced mRNA level of organic solute transporters *Osta* and *Ost β* as well as *Asbt*, and all three treatments increased their levels (Figure 6C).

Moreover, the abundance of cecal bacterial gene *baiJ*, which is responsible for secondary BA synthesis, was increased by FXR deficiency and reduced by *B. infantis* and MO supplementation (Figure 6D). Bacteria-generated butyrate has known anti-inflammatory effects [17, 47]. WD-fed FXR KO mice had reduced copy number of butyrate-generating genes *bcoA* (butyryl-CoA: acetate CoA-transferase) and *buk* (butyrate kinase) in the cecum. MO and *B. infantis* plus MO, but not *B. infantis* alone, were able to increase the abundance of *bcoA* and *buk* (Figure 6D).

3.5. *B. infantis* and MO affect Tgr5 signaling

Because *B. infantis* and MO increased the concentration of endogenous TGR5 ligands LCA and TLCA in FXR KO mice, we hypothesize that the beneficial effect of *B. infantis* and MO in the digestive tract might in part be due to increased TGR5 signaling. Thus, the expression of *Tgr5* and its associated pathways were studied. The data revealed that *B. infantis* and MO supplementation could reverse FXR deficiency-reduced mRNA levels of *Tgr5*, *Glp1r* (glucagon like peptide1 receptor), *PC1/3* (proprotein convertase 1 and 3), *Nos3* (nitric oxide synthase 3), and *Gcg* (preproglucagon) in the ileum (Figure 7). These data revealed the increased TGR5-associated GLP1 signaling in *B. infantis* and MO supplemented mice.

4. Discussion

Bifidobacteria are inhabitants of the human intestine found in the infant gut especially in the breast-fed infants [12]. *Bifidobacteria* regulate immune response and can reduce intestinal inflammation [48]. The anti-inflammatory effects of *Bifidobacteria* have been revealed. For example, *B. infantis* decreases inflammation in necrotizing enterocolitis [3, 49]. *B. infantis* 35624 also reduces LPS-stimulated plasma TNF α and IL6 in healthy volunteers [2]. Furthermore, *B. infantis* DSM15159 improves dextran sodium sulfate-induced acute colitis [50]. In addition, *B. adolescentis* attenuates diet-induced steatohepatitis [51]. Furthermore, *Bifidobacterium* spp. lower gut endotoxin concentration [52] and *B. pseudocatenulatum* CECT 7765 reduces inflammation by reduced IL17A and TNF α [53]. The current study is the first that reveals the anti-inflammatory effect of *B. infantis* in cancer prone NASH caused by dysregulated BA synthesis.

MO has known effect in regulating bacterial colonization and preventing the attachment of pathogens to the intestine [54]. In addition, human MO has been tested in *in vitro* for their anti-inflammatory effect [55]. Human MO inhibited NF- κ B activation, thereby attenuating TNF α - and pathogen-induced inflammation in human intestine [56]. Moreover, MO reduced gut permeability [57]. Our data showed that bovine and human MO had a similar effect. Additionally, a combination of *B. infantis* plus MO gave better outcomes. For examples, in the short-term treatment, *B. infantis* and MO individually reduced hepatic *Il1 β* , *Il6*, *Mcp-1*, *Colla1*, as well as *Ccl20* and a combination *B. infantis* plus MO had higher fold reduction. A similar trend was noted for hepatic *Ccl17*, *Ccl20*, *Cxcl10*, *Ifn γ* , *Icam1*, *Il4* as well as *Timp1*, and *Foxp3* in the long-term treatment. All those encoded cytokines were implicated in hepatitis C virus infection, alcoholic patients, LPS-induced liver injury, and intestinal inflammation [58–60]. In addition, *Icam1* and *Cxcl10* were implicated in lymphocyte adhesion to hepatic sinusoids in NASH patients [61, 62]. Moreover, only *B. infantis* plus MO could increase ileal *Reg3 γ* , which has an anti-microbial effect [63].

In contrast to the anti-inflammatory effect shared by *B. infantis* and MO, *B. infantis* alone, but not MO alone, were effective in reducing hepatic triglyceride as well as hepatic score. When *B. infantis* and MO were used together, they did not change hepatic triglyceride level, but further reduced hepatic cholesterol. These findings suggest their differential effects in regulating lipid metabolism. Previous study showed MO reduced hepatic fat score in high fat diet-fed WT mice [64]. The difference may due to the diet used. The differential effects of *B. infantis* and MO are also demonstrated in other outcomes. Our published data showed

that FXR KO mice have reduced cecal butyrate and increased hepatic inflammation, and butyrate supplementation can treat hepatitis [17]. In the current study, our data showed that MO, but not *B. infantis*, increased the abundance of butyrate-generating *bcoA* and *buk* bacterial genes. These results suggested that MO have other benefits, which are independent from supporting the growth of *B. infantis*.

Our previous data showed that dysregulated BA and gut dysbiosis contribute to hepatic lymphocyte and neutrophil infiltration [15–17]. In this study, we found *B. infantis*, MO, and combination treatment could increase UDCA in the liver and serum, and UDCA is useful to treat NASH [65]. CDCA and TLCA are the endogenous ligands for TGR5 [66]. Activation of TGR5 protects intestinal barrier function, reduces inflammation, improves insulin sensitivity, and stimulates GLP-1 secretion [67, 68]. Moreover, administration of TGR5 agonists INT-777 or INT-767 reduces diet-induced steatosis and insulin resistance [69]. Therefore, *B. infantis* and MO treatment might activate TGR5. This scenario is supported by our findings that TGR5 and its associated signaling pathways including *Glp1r*, *PC1/3*, and *Nos3* etc. were coordinately induced by *B. infantis* and MO. DCA is a secondary BA and has DNA damaging effects [70, 71]. In our study, hepatic DCA was increased in FXR KO mice, and *B. infantis* and MO reduced it. These results are consistent with the changes of bacterial *baiJ* gene in the gut. Moreover, *B. infantis* plus MO were effective in inducing hepatic LCA, which has a known effect in protecting hepatocytes from cholestatic injury [72]. In addition, LCA is a potent pregnane × receptor (PXR) agonist, and induce BA-specific sulfotransferase 2 (Sult2) family to conjugate sulfur to LCA for renal and fecal excretion [73, 74]. Furthermore, increased SULT2A1 might contribute to BA detoxification in *B. infantis* and MO-treated mice [28, 75]. It has been shown that increased hepatic *Sult2a1* or *Sult2a2* expression is an indicator of hepatic sulfonation of BA in mice [76]. *Sult2a8*, which is highly specific for 7 α -hydroxylated bile acids/salts, is reduced due to FXR inactivation [77]. Only *B. infantis* modestly reduced its expression level and the significance of this finding needs to be further investigated. BA homeostasis is tightly regulated. Our data showed, the mRNA and protein level of *Cyp7a1* as well as the mRNA level of *Abcg5* and *Abcg8* were normalized by *B. infantis* and MO supplementation in FXR KO mice suggesting reduced BA synthesis and increased sterols excretion. In addition, *B. infantis* and MO reversed reduced expression of *Osta*, *Ost β* , and *Asbt* in FXR KO mice [78, 79].

In conclusion, *B. infantis* and MO inhibit hepatic inflammation and reduced hepatic fat as well as liver injury in WD-fed FXR KO mice. In addition, synbiotics *B. infantis* and MO normalized dysregulated BA synthesis and are useful to prevent NASH in this mouse model. Moreover, MO increased butyrate-generating bacteria, which have proven useful to prevent NASH. Together, dysbiosis and dysregulated BAs jointly contribute to the development of NASH, and synbiotics can normalize some of those changes and be an effective treatment strategy.

Supplementary Material

Refer to Web version on PubMed Central for supplementary material.

Acknowledgments

Funding: This study is supported by grants funded by National Institutes of Health U01CA179582.

The authors thank Dr. Frank J. Gonzalez (National Cancer Institute, MD, USA) for providing FXR KO mice. We also thank Niki T. DeGeorge for manuscript preparation.

Abbreviations

ALT	alanine transferases
ALP	alkaline phosphatase
BA	bile acid
<i>bcoA</i>	butyryl-coenzyme-A-CoA transferase
<i>buk</i>	butyrate kinase
<i>B. infantis</i>	<i>Bifidobacterium longum</i> subsp. <i>infantis</i>
CA	cholic acid
CDCA	chenodeoxycholic acid
DCA	deoxycholic acid
FXR	farnesoid X receptor
HDCA	hyodeoxycholic acid
KO	knockout
MO	milk oligosaccharides
NASH	nonalcoholic steatohepatitis
SCFA	short chain fatty acid
TGR5	Takeda G-protein coupled receptor 5
TCA	taurocholic acid
TLCA	tauroolithocholic acid
T-α,β-MCA	tauro- α , β -muricholic acid
UDCA	ursodeoxycholic acid
TCDC	taurochenodeoxycholic acid
TDCA	taurodeoxycholic acid
WT	wild type
WD	Western diet

References

1. Bode L. Recent advances on structure, metabolism, and function of human milk oligosaccharides. *J Nutr*. 2006; 136:2127–30. [PubMed: 16857829]
2. Groeger D, O'Mahony L, Murphy EF, Bourke JF, Dinan TG, Kiely B, et al. Bifidobacterium infantis 35624 modulates host inflammatory processes beyond the gut. *Gut microbes*. 2013; 4:325–39. [PubMed: 23842110]
3. Ganguli K, Meng D, Rautava S, Lu L, Walker WA, Nanthakumar N. Probiotics prevent necrotizing enterocolitis by modulating enterocyte genes that regulate innate immune-mediated inflammation. *Am J Physiol Gastrointest Liver Physiol*. 2013; 304:132–41.
4. Miyauchi E, Ogita T, Miyamoto J, Kawamoto S, Morita H, Ohno H, et al. Bifidobacterium longum alleviates dextran sulfate sodium-induced colitis by suppressing IL-17A response: involvement of intestinal epithelial costimulatory molecules. *PLoS one*. 2013; 8:e79735. [PubMed: 24255712]
5. Akay HK, Bahar Tokman H, Hatipoglu N, Hatipoglu H, Siraneci R, Demirci M, et al. The relationship between bifidobacteria and allergic asthma and/or allergic dermatitis: a prospective study of 0–3 years-old children in Turkey. *Anaerobe*. 2014; 28:98–103. [PubMed: 24878320]
6. Kirpich IA, Solovieva NV, Leikhter SN, Shidakova NA, Lebedeva OV, Sidorov PI, et al. Probiotics restore bowel flora and improve liver enzymes in human alcohol-induced liver injury: a pilot study. *Alcohol*. 2008; 42:675–82. [PubMed: 19038698]
7. Asakuma S, Hatakeyama E, Urashima T, Yoshida E, Katayama T, Yamamoto K, et al. Physiology of consumption of human milk oligosaccharides by infant gut-associated bifidobacteria. *J Biol Chem*. 2011; 286:34583–92. [PubMed: 21832085]
8. Aldredge DL, Geronimo MR, Hua S, Nwosu CC, Lebrilla CB, Barile D. Annotation and structural elucidation of bovine milk oligosaccharides and determination of novel fucosylated structures. *Glycobiology*. 2013; 23:664–76. [PubMed: 23436288]
9. Bezkorovainy A. Probiotics: determinants of survival and growth in the gut. *Am J Clin Nutr*. 2001; 73:399–405.
10. Rivero-Urgell M, Santamaria-Orleans A. Oligosaccharides: application in infant food. *Early Human Development*. 2001; 65(Supplement 2):S43–S52. [PubMed: 11755034]
11. Newburg DS, Ruiz-Palacios GM, Morrow AL. Human milk glycans protect infants against enteric pathogens. *Annual review of nutrition*. 2005; 25:37–58.
12. Wickramasinghe S, Pacheco AR, Lemay DG, Mills DA. Bifidobacteria grown on human milk oligosaccharides downregulate the expression of inflammation-related genes in Caco-2 cells. *BMC Microbiol*. 2015; 15:172. [PubMed: 26303932]
13. Hamilton MK, Ronveaux CC, Rust BM, Newman JW, Hawley M, Barile D, et al. Prebiotic milk oligosaccharides prevent development of obese phenotype, impairment of gut permeability, and microbial dysbiosis in high fat-fed mice. *American Journal of Physiology - Gastrointestinal and Liver Physiology*. 2017; 312:G474–G87. [PubMed: 28280143]
14. Taylor SN, Basile LA, Ebeling M, Wagner CL. Intestinal permeability in preterm infants by feeding type: mother's milk versus formula. *Breastfeed Med*. 2009; 4:11–5. [PubMed: 19196035]
15. Sheng L, Jena PK, Liu HX, Kalanetra KM, Gonzalez FJ, French SW, et al. Gender Differences in Bile Acids and Microbiota in Relationship with Gender Dissimilarity in Steatosis Induced by Diet and FXR Inactivation. *Sci Rep*. 2017; 7:1748. [PubMed: 28496104]
16. Jena PK, Sheng L, Liu H-X, Kalanetra KM, Mirsoian A, Murphy WJ, et al. Western Diet-Induced Dysbiosis in Farnesoid X Receptor Knockout Mice Causes Persistent Hepatic Inflammation after Antibiotic Treatment. *Am J Pathol*. 2017; 187:1800–13. [PubMed: 28711154]
17. Sheng LJ, PK, Hu Y, Liu HX, Nagar N, Kalanetra KM, French SW, French SW, Mills DA, Wan YY. Hepatic inflammation caused by dysregulated bile acid synthesis is reversible by butyrate supplementation. *J Pathol*. 2017; 243:431–41. [PubMed: 28892150]
18. Tsuei J, Chau T, Mills D, Wan YJ. Bile acid dysregulation, gut dysbiosis, and gastrointestinal cancer. *Exp Biol Med*. 2014; 239:1489–504.
19. Liu HX, Keane R, Sheng L, Wan YJ. Implications of microbiota and bile acid in liver injury and regeneration. *J Hepatol*. 2015; 63:1502–10. [PubMed: 26256437]

20. Inagaki T, Moschetta A, Lee YK, Peng L, Zhao G, Downes M, et al. Regulation of antibacterial defense in the small intestine by the nuclear bile acid receptor. *Proc Natl Acad Sci U S A*. 2006; 103:3920–5. [PubMed: 16473946]
21. Matsubara T, Li F, Gonzalez FJ. FXR signaling in the enterohepatic system. *Mol Cell Endocrinol*. 2013; 368:17–29. [PubMed: 22609541]
22. Seyer P, Vallois D, Poitry-Yamate C, Schutz F, Metref S, Tarussio D, et al. Hepatic glucose sensing is required to preserve beta cell glucose competence. *J Clin Invest*. 2013; 123:1662–76. [PubMed: 23549084]
23. Ali AH, Carey EJ, Lindor KD. Recent advances in the development of farnesoid X receptor agonists. *Ann Transl Med*. 2015; 3:5. [PubMed: 25705637]
24. Kim I, Morimura K, Shah Y, Yang Q, Ward JM, Gonzalez FJ. Spontaneous hepatocarcinogenesis in farnesoid X receptor-null mice. *Carcinogenesis*. 2007; 28:940–6. [PubMed: 17183066]
25. Yang F, Huang X, Yi T, Yen Y, Moore DD, Huang W. Spontaneous development of liver tumors in the absence of the bile acid receptor farnesoid X receptor. *Cancer Res*. 2007; 67:863–7. [PubMed: 17283114]
26. Liu N, Meng Z, Lou G, Zhou W, Wang X, Zhang Y, et al. Hepatocarcinogenesis in FXR^{-/-} mice mimics human HCC progression that operates through HNF1alpha regulation of FXR expression. *Mol Endocrinol*. 2012; 26:775–85. [PubMed: 22474109]
27. Su H, Ma C, Liu J, Li N, Gao M, Huang A, et al. Downregulation of nuclear receptor FXR is associated with multiple malignant clinicopathological characteristics in human hepatocellular carcinoma. *Am J Physiol Gastrointest Liver Physiol*. 2012; 303:G1245–53. [PubMed: 23042943]
28. Chiang JY. Bile acid metabolism and signaling. *Compr Physiol*. 2013; 3:1191–212. [PubMed: 23897684]
29. Chiang JYL. Bile acid metabolism and signaling in liver disease and therapy. *Liver Res*. 2017; 1:3–9. [PubMed: 29104811]
30. Underwood MA, Kalanetra KM, Bokulich NA, Lewis ZT, Mirmiran M, Tancredi DJ, et al. A comparison of two probiotic strains of bifidobacteria in premature infants. *J Pediatr*. 2013; 163:1585–91. e9. [PubMed: 23993139]
31. Lee H, Cuthbertson DJ, Otter DE, Barile D. Rapid Screening of Bovine Milk Oligosaccharides in a Whey Permeate Product and Domestic Animal Milks by Accurate Mass Database and Tandem Mass Spectral Library. *J Agric Food Chem*. 2016; 64:6364–74. [PubMed: 27428379]
32. Smilowitz JT, Lemay DG, Kalanetra KM, Chin EL, Zivkovic AM, Breck MA, et al. Tolerability and safety of the intake of bovine milk oligosaccharides extracted from cheese whey in healthy human adults. *J Nutr Sci*. 2017; 6:e6. [PubMed: 28620481]
33. Sinal CJ, Tohkin M, Miyata M, Ward JM, Lambert G, Gonzalez FJ. Targeted disruption of the nuclear receptor FXR/BAR impairs bile acid and lipid homeostasis. *Cell*. 2000; 102:731–44. [PubMed: 11030617]
34. Jena PK, Sheng L, Lucente JD, Jin LW, Maezawa I, Wan Y-JY. Dysregulated bile acid synthesis and dysbiosis are implicated in Western diet-induced systemic inflammation, microglial activation, and reduced neuroplasticity. *The FASEB J*. 2018:32.
35. Liu HX, Rocha CS, Dandekar S, Wan YJ. Functional analysis of the relationship between intestinal microbiota and the expression of hepatic genes and pathways during the course of liver regeneration. *J Hepatol*. 2016; 64:641–50. [PubMed: 26453969]
36. Liu HX, Hu Y, Wan YJ. Microbiota and bile acid profiles in retinoic acid-primed mice that exhibit accelerated liver regeneration. *Oncotarget*. 2016; 7:1096–106. [PubMed: 26701854]
37. O’Keefe SJ, Li JV, Lahti L, Ou J, Carbonero F, Mohammed K, et al. Fat, fibre and cancer risk in African Americans and rural Africans. *Nat Commun*. 2015; 6:6342. [PubMed: 25919227]
38. Ridlon JM, Hylemon PB. Identification and characterization of two bile acid coenzyme A transferases from *Clostridium scindens*, a bile acid 7alpha-dehydroxylating intestinal bacterium. *J Lipid Res*. 2012; 53:66–76. [PubMed: 22021638]
39. Louis P, Duncan SH, McCrae SI, Millar J, Jackson MS, Flint HJ. Restricted distribution of the butyrate kinase pathway among butyrate-producing bacteria from the human colon. *J Bacteriol*. 2004; 186:2099–106. [PubMed: 15028695]

40. Louis P, Flint HJ. Development of a semiquantitative degenerate real-time pcr-based assay for estimation of numbers of butyryl-coenzyme A (CoA) CoA transferase genes in complex bacterial samples. *App Environ Microbiol.* 2007; 73:2009–12.
41. Matsuki T, Watanabe K, Fujimoto J, Kado Y, Takada T, Matsumoto K, et al. Quantitative PCR with 16S rRNA-gene-targeted species-specific primers for analysis of human intestinal bifidobacteria. *App Environ Microbiol.* 2004; 70:167–73.
42. Ou J, Carbonero F, Zoetendal EG, DeLany JP, Wang M, Newton K, et al. Diet, microbiota, and microbial metabolites in colon cancer risk in rural Africans and African Americans. *AM J Clin Nutr.* 2013; 98:111–20. [PubMed: 23719549]
43. Jiang C, Xie C, Li F, Zhang L, Nichols RG, Krausz KW, et al. Intestinal farnesoid X receptor signaling promotes nonalcoholic fatty liver disease. *J Clin Invest.* 2015; 125:386–402. [PubMed: 25500885]
44. Kong B, Luyendyk JP, Tawfik O, Guo GL. Farnesoid X receptor deficiency induces nonalcoholic steatohepatitis in low-density lipoprotein receptor-knockout mice fed a high-fat diet. *J Pharmacol Exp Ther.* 2009; 328:116–22. [PubMed: 18948497]
45. Huang F, Wang T, Lan Y, Yang L, Pan W, Zhu Y, et al. Deletion of mouse FXR gene disturbs multiple neurotransmitter systems and alters neurobehavior. *Front Behav Neurosci.* 2015; 9:70. [PubMed: 25870546]
46. Kim I, Ahn SH, Inagaki T, Choi M, Ito S, Guo GL, et al. Differential regulation of bile acid homeostasis by the farnesoid X receptor in liver and intestine. *J Lipid Res.* 2007; 48:2664–72. [PubMed: 17720959]
47. Louis P, Hold GL, Flint HJ. The gut microbiota, bacterial metabolites and colorectal cancer. *Nat Rev Micro.* 2014; 12:661–72.
48. Hardy H, Harris J, Lyon E, Beal J, Foey AD. Probiotics, prebiotics and immunomodulation of gut mucosal defences: homeostasis and immunopathology. *Nutrients.* 2013; 5:1869–912. [PubMed: 23760057]
49. Underwood MA, Arriola J, Gerber CW, Kaveti A, Kalanetra KM, Kananurak A, et al. *Bifidobacterium longum* subsp. *infantis* in experimental necrotizing enterocolitis: alterations in inflammation, innate immune response, and the microbiota. *Pediatr Res.* 2014; 76:326–33. [PubMed: 25000347]
50. Osman N, Adawi D, Molin G, Ahrne S, Berggren A, Jeppsson B. *Bifidobacterium infantis* strains with and without a combination of oligofructose and inulin (OFI) attenuate inflammation in DSS-induced colitis in rats. *BMC Gastroenterol.* 2006; 6:31. [PubMed: 17069659]
51. Reichold A, Brenner SA, Spruss A, Forster-Fromme K, Bergheim I, Bischoff SC. *Bifidobacterium adolescentis* protects from the development of nonalcoholic steatohepatitis in a mouse model. *J Nutri Biochem.* 2014; 25:118–25.
52. Griffiths EA, Duffy LC, Schanbacher FL, Qiao H, Dryja D, Leavens A, et al. In vivo effects of bifidobacteria and lactoferrin on gut endotoxin concentration and mucosal immunity in Balb/c mice. *Dig Dis Sci.* 2004; 49:579–89. [PubMed: 15185861]
53. Moya-Perez A, Neef A, Sanz Y. *Bifidobacterium pseudocatenulatum* CECT 7765 Reduces Obesity-Associated Inflammation by Restoring the Lymphocyte-Macrophage Balance and Gut Microbiota Structure in High-Fat Diet-Fed Mice. *PloS one.* 2015; 10:e0126976. [PubMed: 26161548]
54. Sharon N, Ofek I. Safe as mother's milk: carbohydrates as future anti-adhesion drugs for bacterial diseases. *Glycoconj J.* 2000; 17:659–64. [PubMed: 11421356]
55. Kunz C, Rudloff S. Potential anti-inflammatory and anti-infectious effects of human milk oligosaccharides. *Adv Exp Med Biol.* 2008; 606:455–65. [PubMed: 18183941]
56. Newburg DS, Ko JS, Leone S, Nanthakumar NN. Human Milk Oligosaccharides and Synthetic Galactosyloligosaccharides Contain 3', 4-, and 6'-Galactosyllactose and Attenuate Inflammation in Human T84, NCM-460, and H4 Cells and Intestinal Tissue Ex Vivo. *J Nutr.* 2016; 146:358–67. [PubMed: 26701795]
57. Boudry G, Hamilton MK, Chichlowski M, Wickramasinghe S, Barile D, Kalanetra KM, et al. Bovine milk oligosaccharides decrease gut permeability and improve inflammation and microbial dysbiosis in diet-induced obese mice. *J Dairy sci.* 2017; 100:2471–81. [PubMed: 28131576]

58. Heiseke AF, Faul AC, Lehr HA, Forster I, Schmid RM, Krug AB, et al. CCL17 promotes intestinal inflammation in mice and counteracts regulatory T cell-mediated protection from colitis. *Gastroenterol.* 2012; 142:335–45.
59. Affo S, Morales-Ibanez O, Rodrigo-Torres D, Altamirano J, Blaya D, Dapito DH, et al. CCL20 mediates lipopolysaccharide induced liver injury and is a potential driver of inflammation and fibrosis in alcoholic hepatitis. *Gut.* 2014; 63:1782–92. [PubMed: 24415562]
60. Marra F, Tacke F. Roles for chemokines in liver disease. *Gastroenterol.* 2014; 147:577–94. e1.
61. Shetty S, Lalor PF, Adams DH. Lymphocyte recruitment to the liver: molecular insights into the pathogenesis of liver injury and hepatitis. *Toxicol.* 2008; 254:136–46.
62. Bertola A, Bonnafous S, Anty R, Patouraux S, Saint-Paul MC, Iannelli A, et al. Hepatic expression patterns of inflammatory and immune response genes associated with obesity and NASH in morbidly obese patients. *PLoS one.* 2010; 5:e13577. [PubMed: 21042596]
63. Loonen LM, Stolte EH, Jaklofsky MT, Meijerink M, Dekker J, van Baarlen P, et al. REG3gamma-deficient mice have altered mucus distribution and increased mucosal inflammatory responses to the microbiota and enteric pathogens in the ileum. *Mucosal Immunol.* 2014; 7:939–47. [PubMed: 24345802]
64. Hamilton MK, Ronveaux CC, Rust BM, Newman JW, Hawley M, Barile D, et al. Prebiotic milk oligosaccharides prevent development of obese phenotype, impairment of gut permeability, and microbial dysbiosis in high fat-fed mice. *Am J Physiol Gastrointest Liver Physiol.* 2017; 312:G474–g87. [PubMed: 28280143]
65. Tsuchida T, Shiraiishi M, Ohta T, Sakai K, Ishii S. Ursodeoxycholic acid improves insulin sensitivity and hepatic steatosis by inducing the excretion of hepatic lipids in high-fat diet-fed KK-Ay mice. *Metabolism-Clin Exp.* 2012; 61:944–53.
66. Kawamata Y, Fujii R, Hosoya M, Harada M, Yoshida H, Miwa M, et al. A G protein-coupled receptor responsive to bile acids. *J Biol Chem.* 2003; 278:9435–40. [PubMed: 12524422]
67. Thomas C, Gioiello A, Noriega L, Strehle A, Oury J, Rizzo G, et al. TGR5-Mediated Bile Acid Sensing Controls Glucose Homeostasis. *Cell Metab.* 2009; 10:167–77. [PubMed: 19723493]
68. Maruyama T, Tanaka K, Suzuki J, Miyoshi H, Harada N, Nakamura T, et al. Targeted disruption of G protein-coupled bile acid receptor 1 (Gpbar1/M-Bar) in mice. *J Endocrinol.* 2006; 191:197–205.
69. Pathak P, Liu H, Boehme S, Xie C, Krausz KW, Gonzalez F, et al. Farnesoid X receptor induces Takeda G-protein receptor 5 cross-talk to regulate bile acid synthesis and hepatic metabolism. *J Biol Chem.* 2017; 292:11055–69. [PubMed: 28478385]
70. Bernstein H, Bernstein C, Payne CM, Dvorak K. Bile acids as endogenous etiologic agents in gastrointestinal cancer. *World J Gastroenterol.* 2009; 15:3329–40. [PubMed: 19610133]
71. Delzenne NM, Calderon PB, Taper HS, Roberfroid MB. Comparative hepatotoxicity of cholic acid, deoxycholic acid and lithocholic acid in the rat: in vivo and in vitro studies. *Toxicol Lett.* 1992; 61:291–304. [PubMed: 1641875]
72. Han S, Li T, Ellis E, Strom S, Chiang JY. A novel bile acid-activated vitamin D receptor signaling in human hepatocytes. *Mol Endocrinol.* 2010; 24:1151–64. [PubMed: 20371703]
73. Echchgadda I, Song CS, Oh T, Ahmed M, De La Cruz IJ, Chatterjee B. The xenobiotic-sensing nuclear receptors pregnane X receptor, constitutive androstane receptor, and orphan nuclear receptor hepatocyte nuclear factor 4alpha in the regulation of human steroid-/bile acid-sulfotransferase. *Mol Endocrinol.* 2007; 21:2099–111. [PubMed: 17595319]
74. Pathak P, Cen X, Nichols RG, Ferrell JM, Boehme S, Krausz KW, et al. Intestine farnesoid X receptor agonist and the gut microbiota activate G-protein bile acid receptor-1 signaling to improve metabolism. *Hepatology.* 2018
75. Hofmann AF. Detoxification of lithocholic acid, a toxic bile acid: relevance to drug hepatotoxicity. *Drug metab Rev.* 2004; 36:703–22. [PubMed: 15554243]
76. Alnouti Y. Bile Acid Sulfation: A Pathway of Bile Acid Elimination and Detoxification. *Toxicol Sci.* 2009; 108:225–46. [PubMed: 19131563]
77. Feng L, Yuen YL, Xu J, Liu X, Chan MY, Wang K, et al. Identification and characterization of a novel PPARalpha-regulated and 7alpha-hydroxyl bile acid-preferring cytosolic sulfotransferase mL-STL (Sult2a8). *J Lipid Res.* 2017; 58:1114–31. [PubMed: 28442498]

78. Rao A, Haywood J, Craddock AL, Belinsky MG, Kruh GD, Dawson PA. The organic solute transporter α - β , Ost α -Ost β , is essential for intestinal bile acid transport and homeostasis. *Proc Natl Acad Sci U S A*. 2008; 105:3891–6. [PubMed: 18292224]
79. Jung D, Inagaki T, Gerard RD, Dawson PA, Kliewer SA, Mangelsdorf DJ, et al. FXR agonists and FGF15 reduce fecal bile acid excretion in a mouse model of bile acid malabsorption. *J Lipid Res*. 2007; 48:2693–700. [PubMed: 17823457]

Author Manuscript

Author Manuscript

Author Manuscript

Author Manuscript

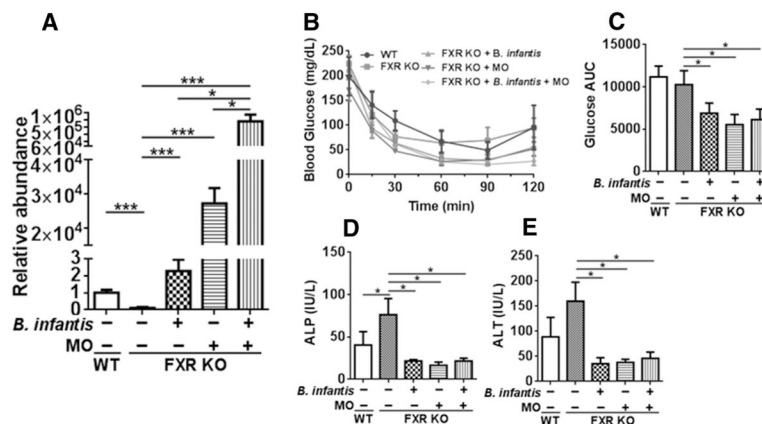


Figure 1. The effects of *B. infantis*, MO, and synbiotics *B. infantis* plus MO in WD-fed FXR KO mice

(A) Relative abundance of *B. infantis*, (B) insulin sensitivity test, (C) area under curve of glucose post insulin injection, (D) serum alkaline phosphatase (ALP), and (E) serum alanine transferase (ALT) levels of WD-fed wild type (WT) mice as well as WD-fed FXR KO mice supplemented with and without *B. infantis*, MO, and *B. infantis* plus MO for 2 months. Data expressed as mean±SD. *n* = 6 per group. **p*<0.05, ****p*<0.001, WT mice compared with FXR KO mice, and untreated FXR KO mice compared with treated FXR KO mice.

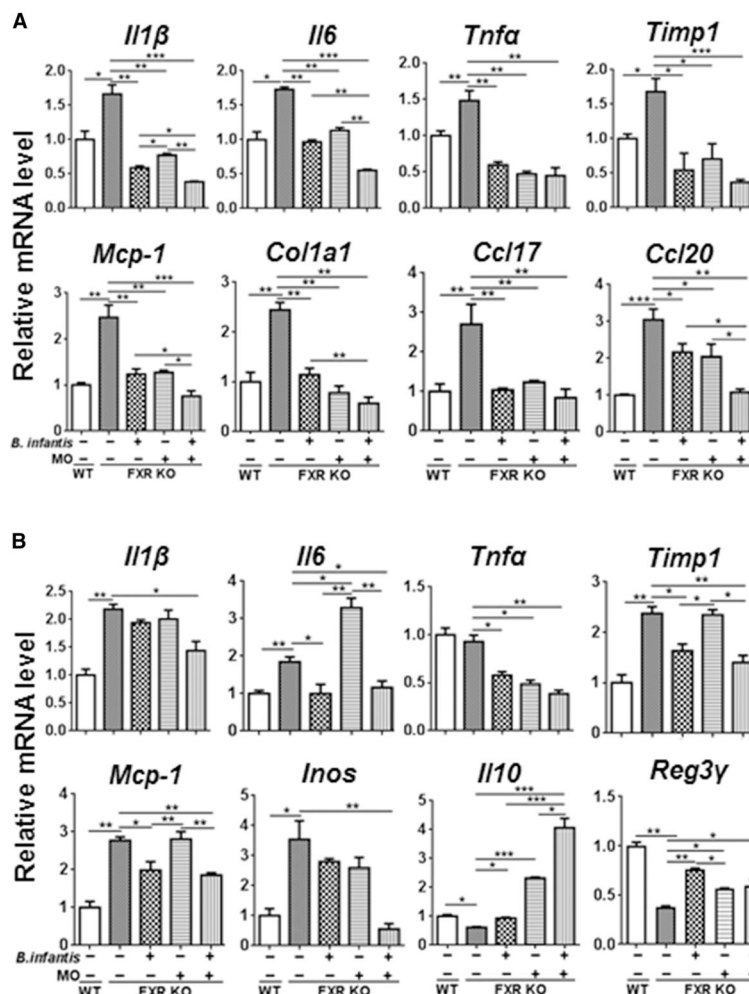


Figure 2. The expression of inflammatory signaling genes in response to *B. infantis* and/or MO treatment

The expression of hepatic genes (A) and ileal genes (B) in diet and gender-matched WT and FXR KO mice supplemented with and without *B. infantis*, MO, and *B. infantis* plus MO for 2 months. Data expressed as mean±SD. n = 6 per group. * $p < 0.05$, ** $p < 0.01$, *** $p < 0.001$, WT mice compared with FXR KO mice, and untreated FXR KO mice compared with treated FXR KO mice.

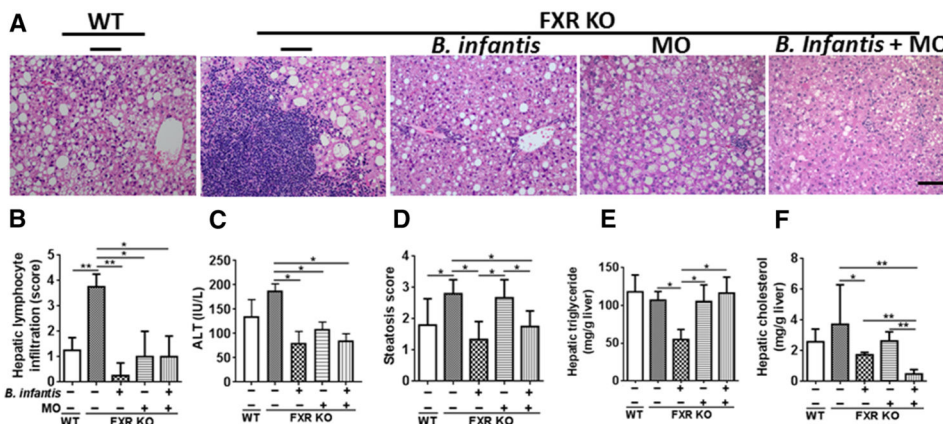


Figure 3. The effects of *B. infantis*, MO and *B. infantis* plus MO on liver pathology (A) Hematoxylin and eosin (H&E) staining of liver, (B) hepatic lymphocyte score, (C) serum ALT level, (D) steatosis score, (E) hepatic triglyceride, and (F) hepatic cholesterol levels of diet and gender-matched mice supplemented with and without *B. infantis*, MO, and *B. infantis* plus MO for 7 months. Data expressed as mean±SD. n = 6 per group. * $p < 0.05$, ** $p < 0.01$, WT mice compared with FXR KO mice, and untreated FXR KO mice compared with treated FXR KO mice.

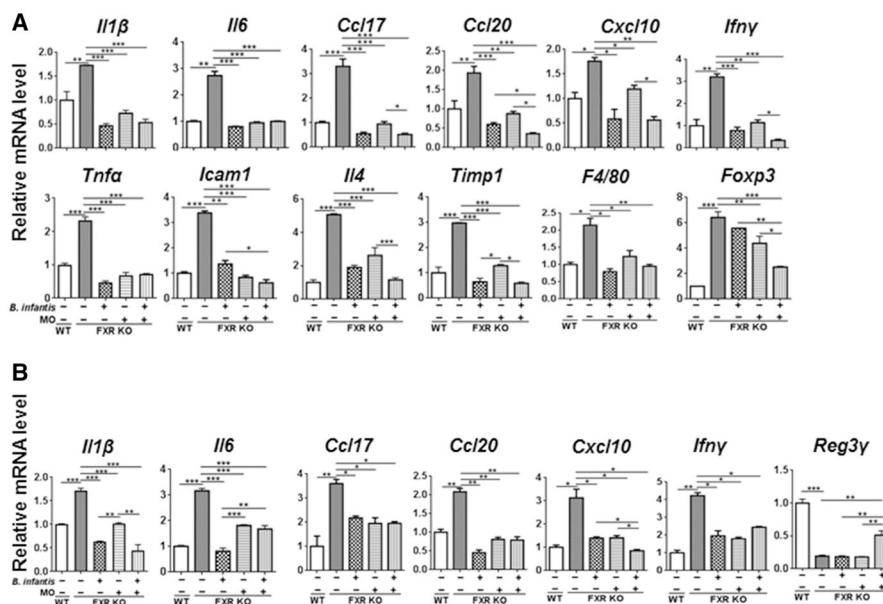


Figure 4. The expression of inflammatory signaling genes in response to *B. infantis* and/or MO treatments

Hepatic (A) and Ileal (B) gene expression in in diet and gender-matched WT and FXR KO mice supplemented with and without *B. infantis*, MO, and *B. infantis* plus MO for 7 months. Data expressed as mean±SD. n = 6 per group. ***p*<0.05, ****p*<0.001, WT mice compared with FXR KO mice, and untreated FXR KO mice compared with treated FXR KO mice.

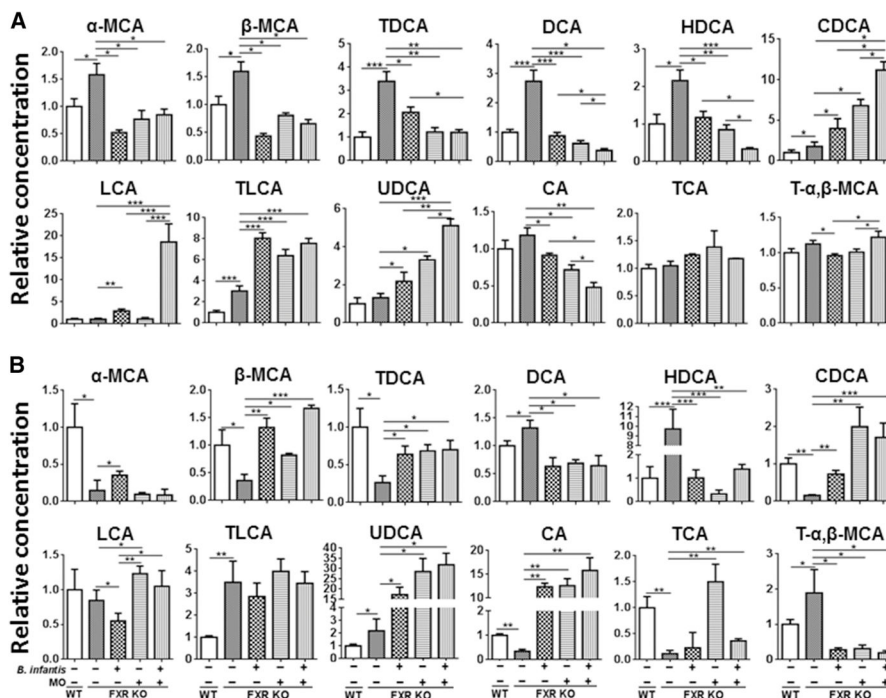


Figure 5. The effects of *B. infantis* and/or MO on hepatic and serum bile acid profiles in WD-fed FXR KO mice

(A) Hepatic and (B) serum bile acid data are expressed as mean \pm SD. n = 6 per group.

* p <0.05, ** p <0.001, *** p <0.0001, WT mice compared with FXR KO mice, and untreated FXR KO mice compared with treated FXR KO mice.

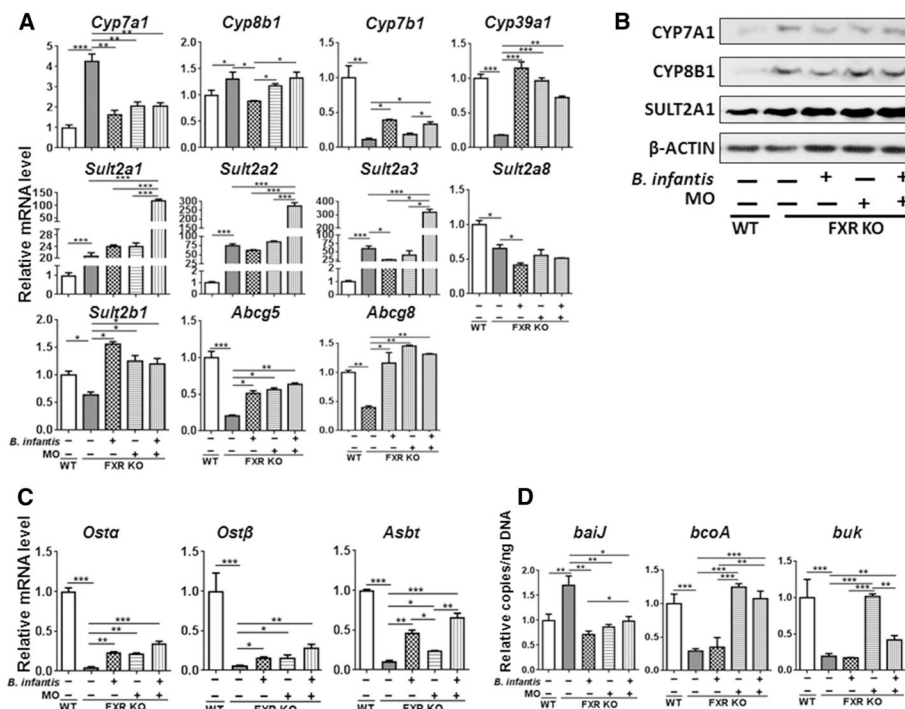


Figure 6. The expression of bile acid homeostasis genes in WD-fed FXR KO mice in response to *B. infantis* and/or MO treatment for 7 months
 (A) Hepatic gene expression, (B) Western blot analysis of indicated hepatic protein levels, (C) ileal gene expression, and (D) targeted functional quantitative PCR analyses of microbial genes. Data expressed as mean±SD. *n* = 6 per group. **p*<0.05, ***p*<0.001, ****p*<0.001, WT mice compared with FXR KO mice, and untreated FXR KO mice compared with treated FXR KO mice.

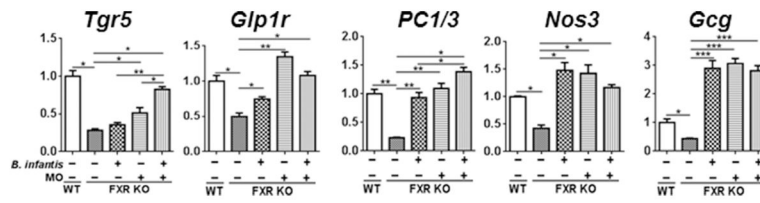


Figure 7. The effects of *B. infantis* and/or MO on TGR5 signaling in WD-fed FXR KO mice. Ileal gene expression of WD-fed WT mice and WD-fed FXR KO mice supplemented with and without *B. infantis* and/or MO for 7 months. Data expressed as mean±SD. n = 6 per group. ***p*<0.05, ****p*<0.001, WT mice compared with FXR KO mice, and untreated FXR KO mice compared with treated FXR KO mice.